NASA Technical Memorandum 105902

Development of Braided Rope Engine Seals

Frank K. Ko, Zhong Cai, and Rajakkannu Mutharasan
Drexel University
Philadelphia, Pennsylvania

and

Bruce M. Steinetz
Lewis Research Center
Cleveland, Ohio

Prepared for the
39th International SAMPE Symposium and Exhibition
sponsored by the
Society for the Advancement of Materials and Process Engineering
Anaheim, California, April 11–14, 1994

National Aeronautics and
Space Administration

DEVELOPMENT OF BRAIDED ROPE ENGINE SEALS

Frank K. Ko, Zhong Cai, and Rajakkannu Mutharasan
Drexel University
Philadelphia, PA 19104

Bruce M. Steinetz
NASA Lewis Research Center
Cleveland, OH 44135

ABSTRACT

In this study, after reviewing current seal design concepts, the potential of textile structures for seal design is examined from the material, structural, and fabrication points of view. Braided structures are identified as potential candidates for hypersonic seal structures because of their conformability and design flexibility. A large family of braided structures using 2-D and 3-D architecture can be designed using well established methods to produce a wide range of braiding yarn orientation for wear resistance as well as seal porosity control. As a first demonstration of the approach, 2-D braided fiberglass seals were fabricated according to a factorial design experiment by varying braiding angles, fractional longitudinal fibers and preload pressure levels. Factorial diagrams and response surfaces were constructed to elucidate the inter-relationship of the braiding parameters as well as the effect of preload pressures on leakage resistance of the seal. It was found that seal resistance is a strong function of fractional longitudinal fiber content. As braiding angle increases, seal leakage resistance increases, especially at high preload pressures and in seals having high proportion of longitudinal fibers.

INTRODUCTION

The primary design function of a hypersonic engine seal is the prevention of hot engine flow path gases and potentially explosive hydrogen/oxygen mixtures from escaping through the seal and damaging engine panel support and articulation systems. Engine chamber sealing can be accomplished in two ways. Selection between the two methods will be based on minimum weight and complexity, maximum reliability and compliance with specific engine design criteria.

The first approach, complete sealing of the chamber, has a high risk factor as the seals cannot be allowed to leak under any circumstance. The second approach, balanced pressure, is more conservative. In this approach, the cavity between two adjacent seals is pressurized slightly above engine flow path pressures. Using positive purging, ensures engine flow path gases such as unburned hydrogen do not get behind the movable panels. With this arrangement, the seals limit purge-gas flow and the purge gas leaking through the seals cools them.

As detailed by Steinetz et al [1], the seal system is expected to meet the following performance requirements:

1 limit coolant purge flow to levels consistent with ambient engine thermal loads;
2 conform to and seal against distorted adjacent engine walls with an estimated deflection of 0.15 inch in an 18 inch span;
3 integrate with panel-hinge seals to form a continuous seal across the hinge;
4 survive the high (200-2800 Btu/ft^2 sec) heat flux environment utilizing minimum coolant resources;
5 resist hydrogen-embrittlement and oxidation;
6 resist sliding abrasion over the engine life (estimated sliding distance is approximately 400 ft.);
7 require minimal actuation forces to overcome seal drag force.

Considering the severity of the operating environments and the critical role seals will play in hypersonic engines, there is a pressing need for systematic development of a design methodology using complementary innovative design concepts. Accordingly, it is the objective of this study to reexamine the performance requirements for the seals and build upon the lessons learned from previous studies as well as exploring new design concepts. Besides meeting the necessary conditions prescribed in the design criteria, it is our specific goal in this multi-phase study to establish a design framework based on an understanding of the interaction of fluid flow and textile seal structures.

In this study, the design concepts and experimental observations of the experimental seals are reported. Guided by these experimental observations, seal designs will be optimized for durability, conformability and manufacturability in subsequent studies.

TEXTILE SEAL CONCEPTS

Textile rope structures have long been used in packing materials and seals. For many years, the only material available for high temperature seals was asbestos because of its high temperature stability, inertness, fine diameter, high strength, and low cost [2]. The health hazard caused by asbestos has created a need for alternate high temperature synthetic fibers. Stimulated by the demands of aerospace applications, a large family of ceramic fibers is now available as shown in Table 1 [3].

An examination of these high temperature fibers reveals that they have high modulus and are extremely brittle. The successful conversion of these fibers into a textile structure and, subsequently, preserving the structural integrity of the seal during handling and end use are of fundamental importance. Besides the intrinsic fiber properties, geometric arrangement such as packing and interlacing plays an important role in the nature of fiber to fiber contact and the contact between fiber and operating surface. Another important consideration in seal design is the resulting porosity of the fibrous structure which dictates the leakage characteristics of the textile seal. In the design of a textile seal, one must consider the structural hierarchy of the textile assembly in addition to the intrinsic property of the fiber.

On the fiber level, as shown by Smith [4], diameter and cross sectional shape have a profound effect on the flexure rigidity and surface area of the fiber. For example, a triangular cross section produces a higher bending stiffness than a circular fiber of the same cross sectional area. On the yarn level or fiber bundle level, the packing density of the fibrous assembly can be modified by the introduction of twist to produce packing densities ranging from 75% to 90%. Different types of fibers with various diameters and cross sectional shapes can also be combined to achieve a particular packing and lubricity effect. On the fabric level the yarn bundles can be organized into open structures such as knits to closely packed structures such as weaves and braids. A comparison of the forming techniques is listed in Table 2. By combining the linear fiber bundles with the various fabric structures, a wide range of structural integrity and fiber packing densities can be achieved.

In general, textile seal design concepts can be organized into the following three categories as shown in Fig. 1.

Multi-layer System. Planar fabric structures are rolled into the desired shape or layers of fabrics are wrapped into a structural shape with an outer tubular structure. Similar effect can also be achieved by placing concentric rings of fabrics over each other.

Core-Sheath System. Structures are made by stuffing tubular fabrics with twisted yarns or parallel fiber bundles.

3-D Integrated System. The yarns are organized into an interconnected three dimensional fiber network by weaving, braiding or orthogonal interlacing. Linear fibrous systems can also be introduced strategically into these 3-D structures.

Of the three families of textile seal concepts listed above, the multi-layer system is perhaps the simplest to assemble; the 3-D system is the most complex but has the highest level of structural integrity. The core-sheath system, on the other hand, provides the highest capacity for the incorporation of longitudinal fibers. Depending on the fiber architecture selected for the seal system, various levels of conformability, abrasion resistance and packing densities can be developed. Of the wide variety of fiber architectures, braided structures provide the highest level of conformability while maintaining a high level of structural integrity and fiber coverage. Ideally, the highest level of packing density can be achieved by packing parallel fibers . In order to provide structural integrity, the introduction of an outer sleeve facilitates handling. An appropriate proportion of sleeve structure to core fibers must address conformability, abrasion resistance, and leakage resistance. When a high level of leakage resistance is required, an integrated structure with high fiber packing density is necessary. While a sleeve/core structure can be created by 2-D over braiding core fiber bundles, fully integrated structures can be produced by 3-D braiding. Braided seal structures will be the focus of our investigation in this study. The subject of braiding and braided structure has been detailed by Ko [5]; only a brief introduction is provided herein.

2-D Braiding. 2-D braiding is an old technology wherein a wide range of braiding angles ($\pm 10^{\circ}$ to $\pm 80^{\circ}$) and highly conformable structures can be produced. The physical and mechanical behavior of braided structures depend upon the fiber orientation, fiber properties and fiber volume fraction. In order to make intelligent design and selection of braids for seals, an understanding of the fiber geometry and volume fraction as a function of processing

parameters is quite necessary. The fiber volume fraction is related to the machine in terms of the number of yarns and the orientation of those yarns. The fiber geometry is related to the machine by orientation of the fibers and final shape. The following is the equation for 2-D braiding calculations [5]:

$$D = \left[\frac{4MN_{ply}A_y}{(\pi V_f \cos\theta) - t_s^2} \right] / 2t_s \qquad (1)$$

where D is the braid diameter, A_y is the cross-sectional area of the yarn, t_s is the sheath thickness, M is number of carriers on the machine, θ is the braiding angle, N_{ply} is number of plies per carrier, and V_f is the fiber volume fraction. With the above equation one can determine the number of carriers required for a given braid diameter to be produced for a specific seal. It should be noted that in addition to the static relationships between braiding angle, θ, braid diameter, D, and number of carriers, M, a dynamic relationship can be established between machine processing parameters and θ and D. With this dynamic relationship, a braid control system can be established to facilitate computer aided manufacturing and assure reproducibility of the seal structure [6].

3-D Braiding. 3-D braiding is an extension of the 2-D braiding technology wherein the fabric is constructed by the intertwining or orthogonal interlacing of two or more yarn systems to form an integral structure. The mechanism of these braiding methods differ from the traditional braiding methods only in the way the carriers are displaced to create the final braid geometry. Instead of moving in a continuous Maypole fashion, as does the square braider, these 3-D braiding methods invariably move the carrier in a sequential, discrete manner, which is quite suitable for adaptation to computer control.

The 3-D braiding system can produce thin and thick structures in a wide variety of complex shapes . The dimension of these structures can be tailored by proper selection of yarn bundle sizes. Fiber orientation can be chosen and 0° longitudinal fibers can be introduced. Where a substantial amount of longitudinal fibers are desired, a 2-step braiding process can be employed to produce a special 3-D braided structure.

The volumetric density and mechanical behavior of a seal depends upon the fabric properties which can be quantified by a knowledge of fiber properties, fiber architecture, fiber orientation and fiber volume fraction. The following is the equation for 3-D braided structure calculations [5]:

$$V_f = \frac{N_y D_y}{9x10^5 \rho_f A_s \cos\theta'} \qquad (2)$$

where N_y is the total number of yarns in the fabric, ρ_f is the fiber density, A_s is the cross-sectional area of the seal, D_y is the yarn linear density in denier which represents grams per 9000 meters, and θ' is the yarn surface angle. Using the above equation, one can easily

determine the total number of yarns required to make a fabric with a given fiber volume fraction, V_f and cross sectional area, A_c, when fiber density, ρ_f (g/cc), yarn linear density, D_y (denier); and yarn surface angle, θ' (deg), are specified. The factor of 9×10^5 is used for the units involved.

EXPERIMENTS

In this initial study and with the consideration of the maturity of 2-D braiding technology, our investigation focuses on 2-D braided structures. Guided by the governing equations of braided structures, a series of controlled experiments were designed and performed to evaluate the design concept. This section describes the selection of design parameters, experiment design and experimental procedures.

Design of Experiment. From equation (1), it can be seen that braiding angle and yarn bundle size are key parameters affecting the volume fraction or porosity of the braided seal. Depending on the pressure applied to the seal structure, the fiber volume fraction of the seal will be further modified. In order to develop a sense of the interrelationships of the seal structural parameters and testing conditions, the effect of braiding angle θ, percentage of longitudinal or core yarn L, and preload pressure level P were investigated. To facilitate assessment of the relative significances and the interaction effect of the structural parameters and test conditions, a two level, three factor design-factorial experiment was planned as shown in Table 3. The symbol [-] indicates low level while symbol [+] represents high level.

Specimen Fabrication. Four sets of braided seal specimens were prepared on a 24 carrier Wardwell braiding machine according to the experimental design. Multiples of 812 denier E-glass yarns were used for braider and core (0°) yarns to produce various configuration of the seal. Braid angle and braiding details are given in Tables 4 and 5. Calculated fiber volume fractions for selected seals are given in Table 4.

The experimental seal specimen, as depicted in Figure 1, consists of a braided sheath and a fiber core. The braided sheath was formed by braiding over a bundle of parallel filaments. The number of braid layers is one of the parameters which need to be optimized for flow resistance, conformability, and durability. Other parameters, such as number of yarn carriers, thickness of braiding yarns, braiding angles, and yarn covering factor, were determined from the dimensions of seal specimen to produce an optimal structure.

As illustrated in Fig 2, the seal specimen was transformed into a square (approximately 0.5 inch) shape with round corners after the application of preload pressure. With a known (or estimated) thickness of braid sheath and diameter of fibers at the core, the number of core fibers can be calculated from the required fiber volume fraction.

Seal Testing. Seals were tested in a fixture designed and constructed at NASA Lewis Research Center. Seal testing was carried out at Drexel University using the experimental setup shown in Fig. 2.

After the seal was placed in the seal channel, the cover plate (representing the adjacent engine panel) was fastened into place. A proper level of preload pressure was then applied to the specimen. Two levels of preload pressure (80 and 130 psi) were used in the experiments, and were applied with an inflatable bladder. After the preload pressure P reached a stable level (usually within 2-3 minutes), the inlet pressure p_i was noted before recording the gauge flow Q_g indicated in the flow meter.

A seal resistance is defined as

$$R = \frac{p_i^2 - p_o^2}{\dot{M}/L_s} \tag{3}$$

where p_i is the inlet pressure, p_o is the outlet pressure, $\dot{M}$ is the mass flux of the leakage gas, and L_s is the seal length. This seal resistance is used in the follwing comparisons.

RESULTS AND ANALYSIS

For the purposes of calibrating the test apparatus, two gases having a wide difference in density (air, 0.076 lb/ft^3 at 70 °F and 14.7 psia and helium, 0.0105 lb/ft^3 at 70°F and 14.7 psia) were used for the seal tests. In order to check the linearity of the dependency of seal flow resistance on seal parameters and preload pressures, additional experiments were carried out at intermediate levels of braiding angle (30°) and longitudinal fibers (55%).

The experimental flow resistances of the braided seals to air and helium is listed in Table 5. These results can be analyzed in terms of factorial diagrams as shown in Figures 3 and 4. Based on the coordinates indicated by the symbols [+], [0], and [-], representing high, intermediate, and low level respectively, one can establish the dependence of seal resistance on seal structural parameters and preload pressures. In general, it can be seen that the seals have higher resistance to helium than air. This is to be expected since helium has higher kinematic viscosity than air. Seal resistance increases as the preload pressure increases. The effect of preload pressure seems to be more significant in seals having a higher percentage of longitudinal fibers. Similar trends are also evident in the effect of braiding angle. At low longitudinal fiber fraction, the effect of braiding angle on seal resistance is insignificant, whereas at high longitudinal fiber fraction, increasing braiding angle brings about a significant increase in seal resistance. It appears that the combination of high braiding angle with a high percentage of longitudinal fibers results in the highest level of seal resistance. This effect is even more pronounced when the seal is tested under high preload pressure.

Making use of this controlled factorial experiment, one can generate response surfaces using the well established mathematical statistics methodologies [7]. The response surfaces are based on the empirical equations for seal resistance to air (R_A) and helium (R_H), and are given below:

$$R_A = 0.88 + 0.16X_1 + 0.41X_2 + 0.16X_1X_2 + 0.20X_3 + 0.12X_1X_3 + 0.17X_2X_3 + 0.12X_1X_2X_3$$

$$R_H = 8.03 + 2.40X_1 + 4.33X_2 + 2.35X_1X_2 + 2.05X_3 + 0.88X_1X_3 + 1.50X_2X_3 + 0.88X_1X_2X_3 \tag{4}$$

where the variables are:

$$x_1 = 2\left(\frac{\theta - 27.5}{35}\right)$$

$$x_2 = 2\left(\frac{L - 0.55}{0.40}\right)$$

$$x_3 = 2\left(\frac{P - 105}{50}\right) \qquad (5)$$

In these relations x_1, x_2, and x_3 represent braiding angle, fraction of longitudinal fibers, and preload pressure respectively. From these response curves, one can examine a detailed response profile of the different faces of the factorial diagrams shown in Fig. 3 and Fig. 4. Although the validity of the response surface is limited to the experimental region, the extrapolated area does provide a broader picture as a guide for future theoretical modeling and exploration of new design concepts. Based on the response surface analysis, the theoretical minima and maxima of the R values for the braided seals are summarized in Table 6. This analysis further confirms that high braiding angle and high fractional longitudinal fiber surface are preferred in the design of low leakage seals.

CONCLUSIONS

In this study the potential of textile structures for seal design is examined from the the material, structural, and fabrication points of view. Braided structures are identified as potential candidates for hypersonic seal structures because of their conformability and tailorable flow characteristics. A large family of braided structures using 2-D and 3-D architecture can be designed using well established design methods to produce a wide range of braiding yarn orientation for wear resistance as well as seal porosity control. As a first demonstration of concept, 2-D braided fiberglass seals were fabricated according to a factorial experiment by varying braiding angles, fractional longitudinal fibers and preload pressure levels. Factorial diagrams and response surfaces were constructed to elucidate the interrelationship of the braiding parameters as well as the effect of preload pressure on the leakage resistance of the seal. It was found that seal resistance is a strong function of fractional longitudinal fiber. As braiding angle increases, seal resistance increases, especially at high preload pressure and in seals having high proportions of longitudinal fibers.

The experimental observations provide a helpful basis for formulating theoretical modeling of seal performance as well as the development of new design concepts. Future efforts will focus on flow modeling, modeling of preload pressure effects, as well as optimization of the seal design to include seal durability.

REFERENCES

1. Steinetz, B.M., DellaCorte, C., and Sirocky, P.J., "On the Development of Hypersonic Engine Seals", NASA TP-2854, 1988.

2. Handbook of Asbestos Textiles, Asbestos Textile Institute, Pompton Lakes, New Jersey, 1967.

3. Ko, F.K. , "Preform Fiber Architecture for Ceramic Matrix Composites", Am. Cer. Soc. Bull., Vol. 68. No.2, Feb. 1989.

4. Smith, D.H., "Textile Fibers - An Engineering Approach to Their Properties and Utilization", Edgar Marburg Lectures, ASTM, 1944.

5. Ko, F.K., "Braiding", Engineering Materials Handbook, Vol. 1, Composites, Edited by Reinhart, T.J., American Society for Materials International, Metal Park, OH, 1988.

6. Yang, G., Pastore, C.M., Tsai, Y.J., Soebroto, H.B., and Ko, F.K., "CAD/CAM of Braided Preforms for Advanced Composites," Proceedings, Advanced Composites III - Expanding the Technology, ASM International, Metals Park, Ohio, 1987, pp. 103-107.

7. Myers, R.H., Response Surface Methodology, Allyn and Bacon, Inc, Boston, 1971.

Table 1. Properties of Candidate Fibers for Ceramic Matrix Composites

Fiber (Manufacturer)	Density (g/cc)	Strength MPa (ksi)	Modulus GPa(Msi)	Diameter (mm)	Maximum Use Temp (°C)
Alumina					
Fiber FP (duPont)	3.9	1.38 (200)	380 (55)	21	1316
PRD166 (duPont)	4.2	2.07 (300)	380 (55)	21	1400
Sumitomo	3.9	1.45 (210)	190 (28)	17	1249
Mullite					
Nextel 440 (3M)	3.1	2.7 (250)	186 (30)	12 & 8	1426
Mullite/Gls					
Nextel 312 (3M)	2.7	1.55 (225)	150 (22)	12 & 8	1204
b-SiC Multifilament					
Nicalon (Nippon Carbon)	2.55	2.62 (380)	193 (28)	10	1204
SiTiCO					
Tyranno (UBE)	2.5	2.76 (400)	193 (28)	10	1300
Si_3N_4					
TNSN (Tonen)	2.5	3.3 (362)	296 (43)	10	1204
SiC Whisker					
VLS (Los Alamos)	3.2	8.3 (1200)	580 (84)	4-7	1400
SiC Monofilament					
SCS-6 (Textron)	3.05	3.45 (500)	410 (60)	140	1299
Sigma (Berghof)	3.4	3.45 (500)	410 (60)	100	1259
Pure Fused Silica					
Astroquartz (J.P. Stevens)	2.2	3.45 (500)	69 (10)	9	993
Graphite					
T300R (Amoco)	1.8	2.76 (400)	276 (40)	10	>1648*
T40R (Amoco)	1.8	3.45 (500)	276 (40)	10	>1648*

*Non-oxidizing environments

Table 2: Comparison of Yarn-to-Fabric Formation Techniques

	Basic Direction of Yarn Introduction	Basic Formation Technique
Weaving	Two (0°/90°) (warp and fill)	Interlacing (by selective insertion of 90° yarns into 0° yarn system)
Braiding	Multi-dimensional (Machine Direction)	Intertwining (position displacement)
Knitting	One (0° or 90°) (warp or fill)	Interlooping (by drawing loops of yarns over previous loops)
Nonwoven	Three or more (orthogonal)	Mutual fiber placement

Table 3: Factorial Design

	Factor Symbols			Actual Factors		
Trial	θ	**L**	**P**	θ (deg)	**L** (%)	**P** (psig)
1	-	-	-	10	35	80
2	+	-	-	45	35	80
3	-	+	-	10	75	80
4	+	+	-	45	75	80
5	-	-	+	10	35	130
6	+	-	+	45	35	130
7	-	+	+	10	75	130
8	+	+	+	45	75	130

Table 4: Braid Angle and Braiding Details

Sample No.	Braid Angle (deg)	0° Yarn (%)	Fiber Volume Fraction (V_f) (%)
A-1	45	35	52.4
C-1	10	75	51.1
G-1	45	75	54.7
J-1	10	75	-

Table 5: Measured Seal Resistance

Sample No.	Factors			Factor Symbols			R_{Air}	R_{Helium}
	θ (deg)	L (%)	P (psig)	θ (deg)	L (%)	P (psig)	$\left(\frac{psi^2/lb}{ft\text{-}sec}\right)\times 10^6$	
A-1-P1	10	35	80	-	-	-	0.44	3.40
C-1-P1	45	35	80	+	-	-	0.45	3.20
G-1-P1	10	75	80	-	+	-	0.83	5.80
I-1-1P1	45	75	80	+	+	-	1.00	11.80
A-1-P2	10	35	130	-	-	+	0.49	4.20
C-1-P2	45	35	130	+	-	+	0.50	4.30
G-1-P2	10	75	130	-	+	+	1.10	9.40
I-1-1P2	45	75	130	+	+	+	2.20	22.40
B-1-P1	30	35	80	0	-	-	0.44	3.20
D-1-P1	45	55	80	+	0	-	0.57	3.90
F-1-P1	10	55	80	-	0	-	1.30	11.80
H-1-P1	30	75	80	0	+	-	0.83	5.80
B-1-P2	30	35	130	0	-	+	0.49	3.50
D-1-P2	45	55	130	+	0	+	0.67	5.60
F-1-P2	10	55	130	-	0	+	2.20	22.40
H-1-P2	30	75	130	0	+	+	1.10	9.40
E-1-P1	30	55	80	0	0	-	0.79	5.00
E-1-P2	30	55	130	0	0	-	0.79	7.40

Table 6: Theoretical Maxima and Minima of Seal Resistance

	θ (deg)	L (%)	P (psig)	R_{Air}	R_{Helium}
				$\left(\frac{psi^2/lb}{ft\text{-}sec}\right)\times 10^6$	
Min	10	35	80	0.44	3.1
Max	80	95	80	1.52	25.0
Min	10	35	130	0.50	4.2
Max	80	95	130	4.76	51.0

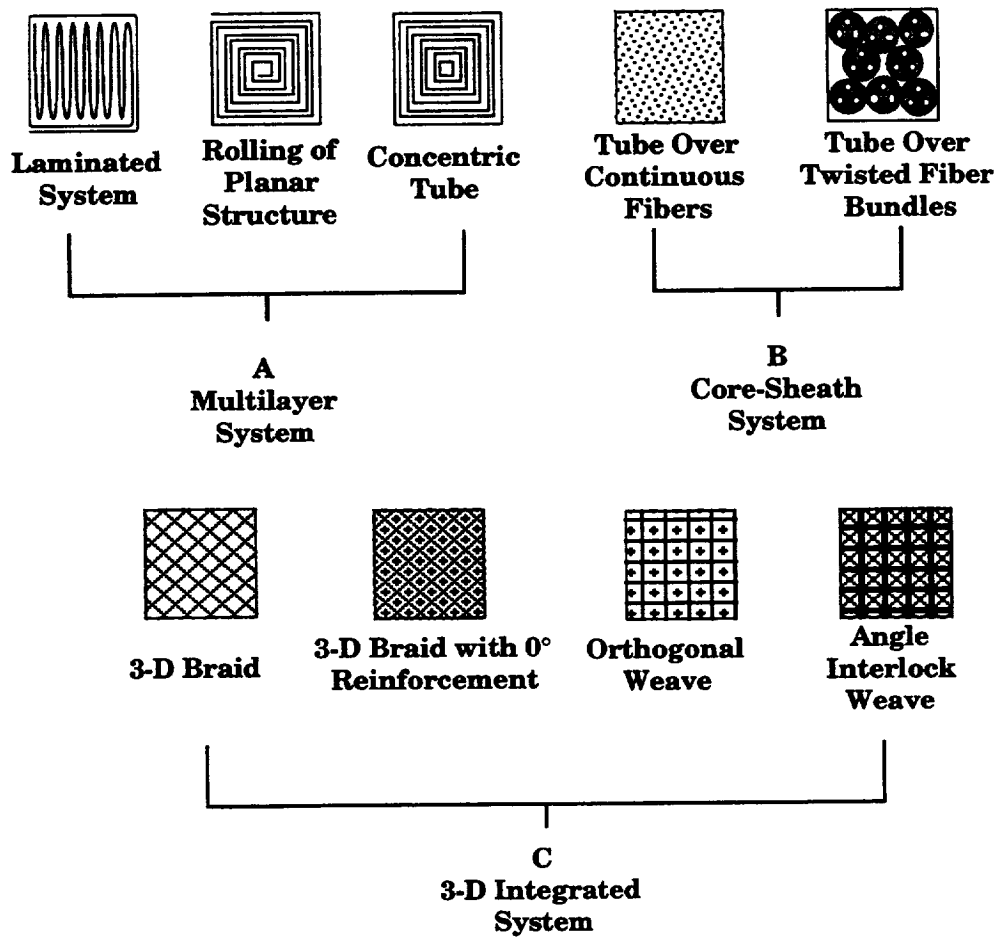

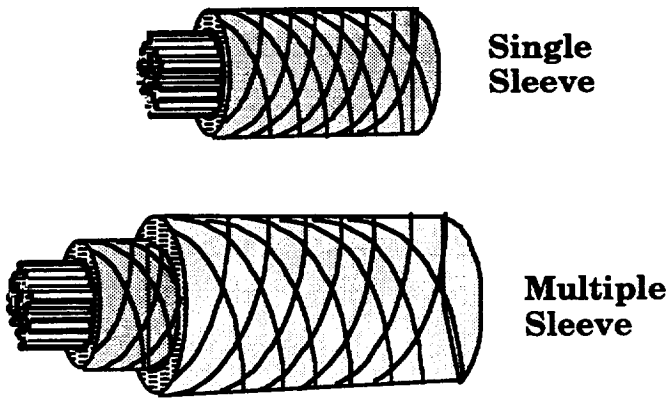

Figure 1.—Textile seal design concepts.

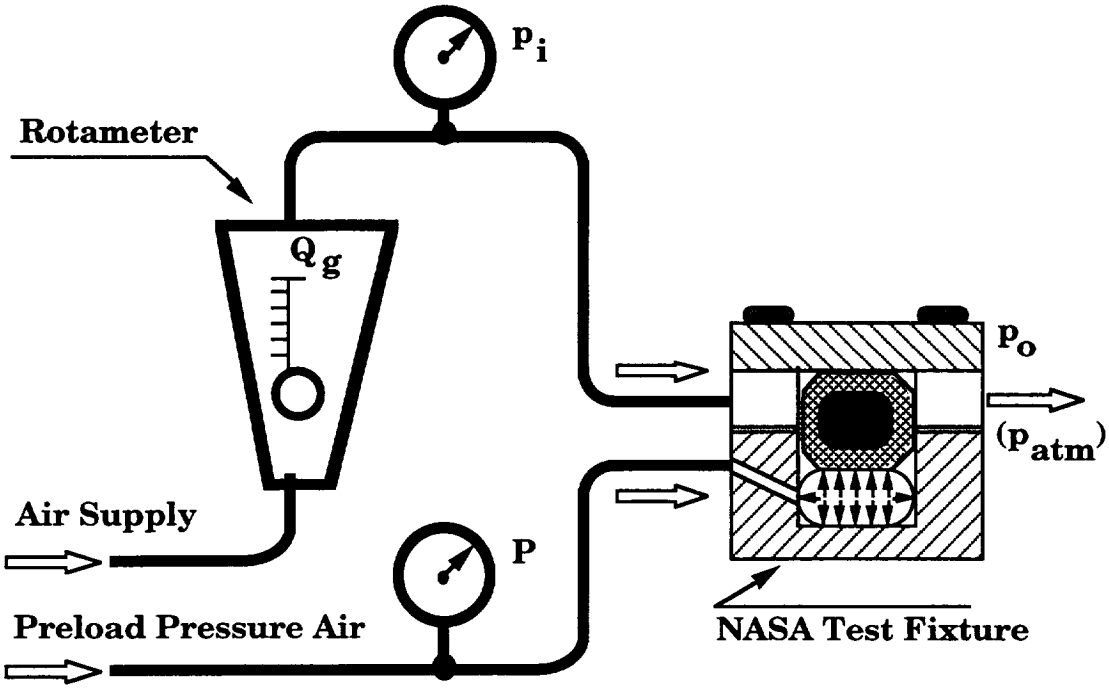

Figure 2.—Experimental apparatus and setup.

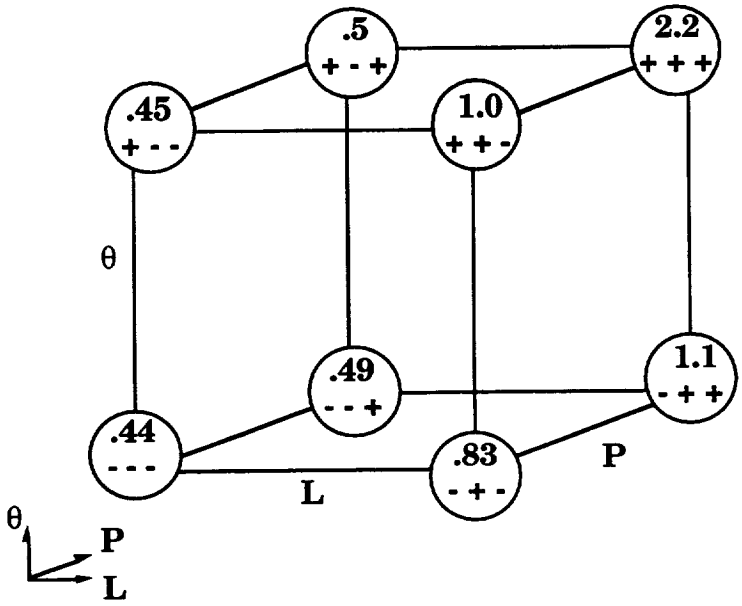

Figure 3.—Factorial diagram - air.

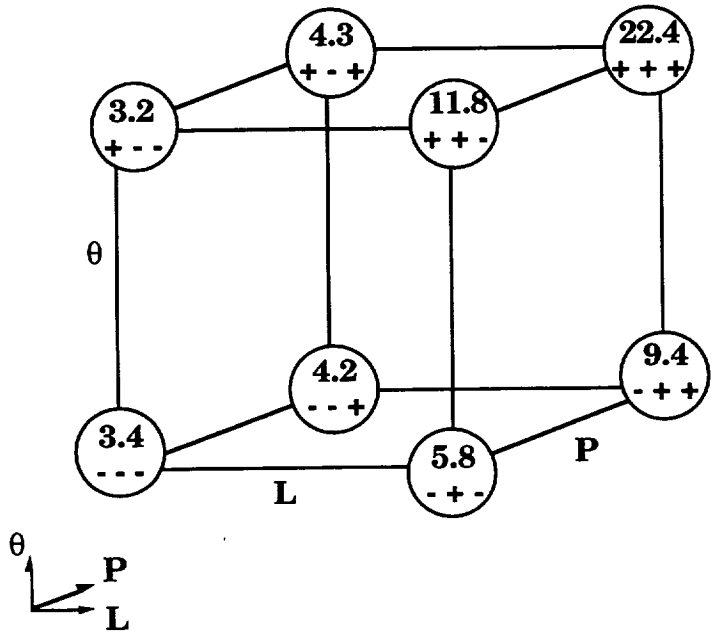

Figure 4.—Factorial diagram - helium.

REPORT DOCUMENTATION PAGE

Form Approved
OMB No. 0704-0188

1. AGENCY USE ONLY (*Leave blank*)	2. REPORT DATE	3. REPORT TYPE AND DATES COVERED
	February 1994	Technical Memorandum

4. TITLE AND SUBTITLE

Development of Braided Rope Engine Seals

5. FUNDING NUMBERS

WU–763–22–2J

6. AUTHOR(S)

Frank K. Ko, Zhong Cai, Rajakkannu Mutharasan, and Bruce M. Steinetz

7. PERFORMING ORGANIZATION NAME(S) AND ADDRESS(ES)

National Aeronautics and Space Administration
Lewis Research Center
Cleveland, Ohio 44135–3191

8. PERFORMING ORGANIZATION REPORT NUMBER

E–8639

9. SPONSORING/MONITORING AGENCY NAME(S) AND ADDRESS(ES)

National Aeronautics and Space Administration
Washington, D.C. 20546–0001

10. SPONSORING/MONITORING AGENCY REPORT NUMBER

NASA TM–105902

11. SUPPLEMENTARY NOTES

Prepared for the 39th International SAMPE Symposium and Exhibition sponsored by the Society for the Advancement of Materials and Process Engineering, Anaheim, California, April 11–14, 1994. Frank K. Ko, Zhong Cai, and Rajakkannu Mutharasan, Drexel University, Philadelphia, Pennsylvania 19104; and Bruce M. Steinetz, NASA Lewis Research Center. Responsible person, Bruce M. Steinetz, organization code 5230, (216) 433–3302.

12a. DISTRIBUTION/AVAILABILITY STATEMENT

Unclassified – Unlimited
Subject Category 37

12b. DISTRIBUTION CODE

13. ABSTRACT ***(Maximum 200 words)***

In this study, after reviewing current seal design concepts, the potential of textile structures for seal design is examined from the material, structural, and fabrication points of view. Braided structures are identified as potential candidates for hypersonic seal structures because of their conformability and design flexibility. A large family of braided structures using 2-D and 3-D architecture can be designed using well established methods to produce a wide range of braiding yarn orientation for wear resistance as well as seal porosity control. As a first demonstration of the approach, 2-D braided fiberglass seals were fabricated according to a factorial design experiment by varying braiding angles, fractional longitudinal fibers and preload pressure levels. Factorial diagrams and response surfaces were constructed to elucidate the inter-relationship of the braiding parameters as well as the effect of preload pressures on leakage resistance of the seal. It was found that seal resistance is a strong function of fractional longitudinal fiber content. As braiding angle increases, seal leakage resistance increases, especially at high preload pressure.

14. SUBJECT TERMS	15. NUMBER OF PAGES
Seals; Braid; Leakage flow	16
	16. PRICE CODE: A03

17. SECURITY CLASSIFICATION OF REPORT	18. SECURITY CLASSIFICATION OF THIS PAGE	19. SECURITY CLASSIFICATION OF ABSTRACT	20. LIMITATION OF ABSTRACT
Unclassified	Unclassified	Unclassified	